

Controlling the synthesis SrMoO₄ nanostructures and investigation its photocatalyst application

S. Mostafa Hosseinpour-mashkani¹ · Ali Sobhani-Nasab¹ · Meraat Mehrzad²

Received: 14 November 2015 / Accepted: 6 February 2016 / Published online: 11 February 2016
© Springer Science+Business Media New York 2016

Abstract In this paper, strontium molybdate (SrMoO₄) nanostructures were synthesized via a sonochemical method based on the reaction between strontium (II) nitrate and ammonium heptamolybdate tetrahydrate in water. Capping agents are frequently used in colloidal synthesis to inhibit nanoparticle overgrowth and aggregation as well as to control the structural characteristics of the resulted nanoparticles in a precise manner; therefore, glucose and lactose were applied as capping agents. Besides, the effect of glucose and lactose on the morphology and size of final products were investigated by SEM analysis. According to the vibrating sample magnetometer, SrMoO₄ nanostructures indicated a ferromagnetic behavior at room temperature. To evaluate the catalytic properties of nanocrystalline SrMoO₄, the photocatalytic degradations of methyl orange under ultraviolet light irradiation were carried out. The structural, morphological, magnetic, and optical properties of as-obtained products were characterized by techniques such as XRD, SEM, EDX, VSM, and UV–Vis spectroscopy.

1 Introduction

Nanostructures have gained much attention among materials, because the nanocrystal properties not only depend on their composition but also depend on their size, shape,

and size distribution [1–7]. In recent years, tungstates and molybdates are materials that have attracted the interest of many technological fields and scientific areas owing to their wide potential to industrial application, including optic fiber, humidity sensor, catalysts, scintillation detector, solid-state lasers, photoluminescent devices, microwave applications and so on [8–17]. These materials have been prepared in both powder and film forms by means of several technologies, such as spray pyrolysis, pulsed laser deposition, RF-magnetron sputtering, and sol–gel method [18–22]. However, these methods generally require expensive and sophisticated equipments, high temperatures for a long time, expensive precursors and high consumption of electric energy [23]. A possible alternative for reduction of these factors can be the use of sonochemical method. Orthomolybdates are very interesting materials due to their applications. Strontium molybdate (SrMoO₄) is a prominent member of this family. It has attracted particular interest as host for lanthanide-active lasers as well as scintillator and photocatalytic material [24–26]. SrMoO₄ crystallizes in the so-called scheelite structure (scheelite = CaWO₄) [27] which belongs to the tetragonal space group (SG) I4_{1/a}. There are some methods for SrMoO₄ preparation which involve co-precipitation [28], solid state reaction method [29], and combining sol–gel and solid-state route [30]. Among various methods for the preparation of nanostructures, ultrasonic method is more promising in terms of low cost, simply control the shape and particle size, low processing temperature, simplicity, and potential for large-scale production. Recently, the ultrasonic process as a fast, convenient, and economical method has been widely used to generate novel nanostructured materials under ambient conditions [31, 32]. It is widely accepted that the properties of nanomaterials have a close relationship with their

✉ Ali Sobhani-Nasab
ali.sobhaninasab@gmail.com

¹ Young Researchers and Elites Club, Arak Branch, Islamic Azad University, Arak, Iran

² Department of Analytical Chemistry, Faculty of Chemistry, University of Kashan, Kashan 87317-51167, Iran

morphology, size, size distribution, crystallinity, and control over the morphology and size of inorganic materials at micro and nano scale level is an important goal; therefore, in this paper we investigate the effect of glucose and lactose as capping agents on the morphology and particle size of SrMoO_4 nanostructures with aid of sonochemical method. In addition, the efficiency of the SrMoO_4 nanostructures as a photocatalyst for the decolorization of methyl orange (MO) using ultraviolet light irradiation has been evaluated.

2 Experimental

2.1 Characterization

All the chemicals used in this method were of analytical grade and used as-received without any further purification. Ultrasonic irradiation was accomplished using a high-intensity ultrasonic probe (Sonicator 3000; Bandeline, MS 72, Germany, Tihorn, 20 kHz, 60 W cm^{-2}) immersed directly in the reaction solution. X-ray diffraction (XRD) pattern was recorded by a Philips-X'PertPro, X-ray diffractometer using Ni-filtered Cu $K\alpha$ radiation at scan range of $10 < 2\theta < 80$. Scanning electron microscopy (SEM) images were obtained on LEO-1455VP equipped with an energy dispersive X-ray spectroscopy. The electronic spectra of the zinc tungstate were obtained on a Scinco UV-Vis scanning spectrometer (Model S-10 4100). The energy dispersive spectrometry (EDS) analysis was studied by XL30, Philips microscope. The magnetic measurement of

Table 1 Reaction conditions for SrMoO_4 nanostructures

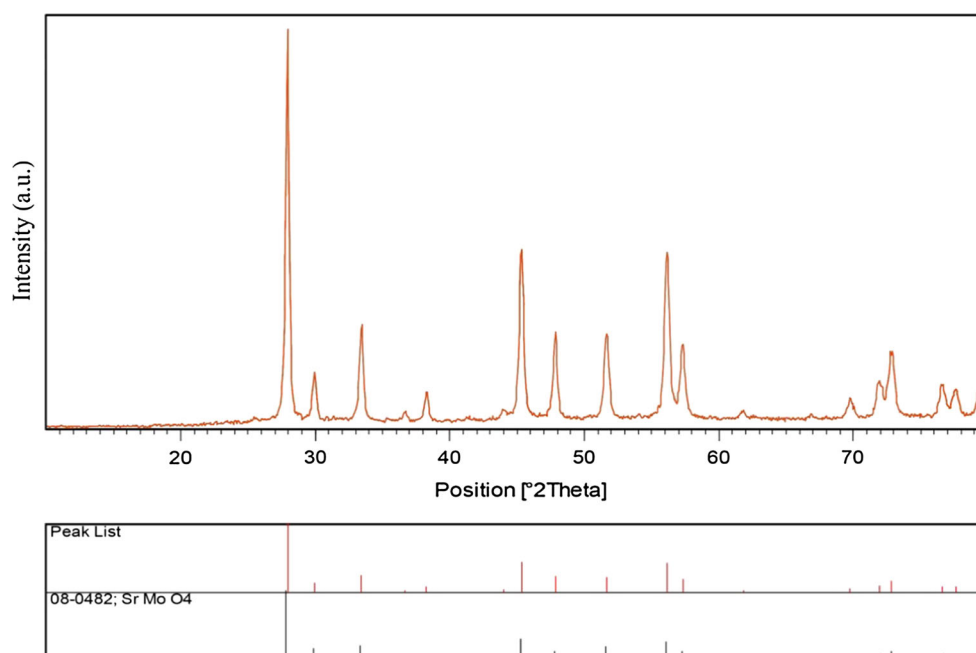
Sample no	Power (W)	Capping agent	Degradation (%)
1	70	–	71
2	70	Lactose	62
3	70	Glucose	51

samples were carried out in a vibrating sample magnetometer (VSM) (Meghnatis Daghigh Kavir Co.; Kashan Kavir; Iran) at room temperature in an applied magnetic field sweeping between $\pm 10,000$ Oe.

2.2 Synthesis of SrMoO_4 nanostructures

At the first step, the appropriate amount of $\text{Sr}(\text{NO}_3)_2$ (0.60 gr) and $(\text{NH}_4)_6\text{Mo}_7\text{O}_{24}\cdot 4\text{H}_2\text{O}$ (0.50 gr) was dissolved in 20 ml of distilled water separately. Then, 0.5 gr of lactose as natural surfactant was added to the $\text{Sr}(\text{NO}_3)_2$ solution under constant stirring. Afterwards, the final solution was loaded into a beaker and the reaction was carried out in an ultrasonic digestion system at 70 W for 15 min. Subsequently, during the sonication, the solution of $(\text{NH}_4)_6\text{Mo}_7\text{O}_{24}\cdot 4\text{H}_2\text{O}$ was added into the above solution. After irradiation, the system was allowed to cool to room temperature naturally, the obtained precipitate was collected by filtration, and washed with absolute ethanol and distilled water several times. Finally, the product was dried in vacuum at 90 °C for 2 h. Reaction conditions are listed in Table 1.

Fig. 1 XRD pattern of SrMoO_4 nanostructures (sample 1)



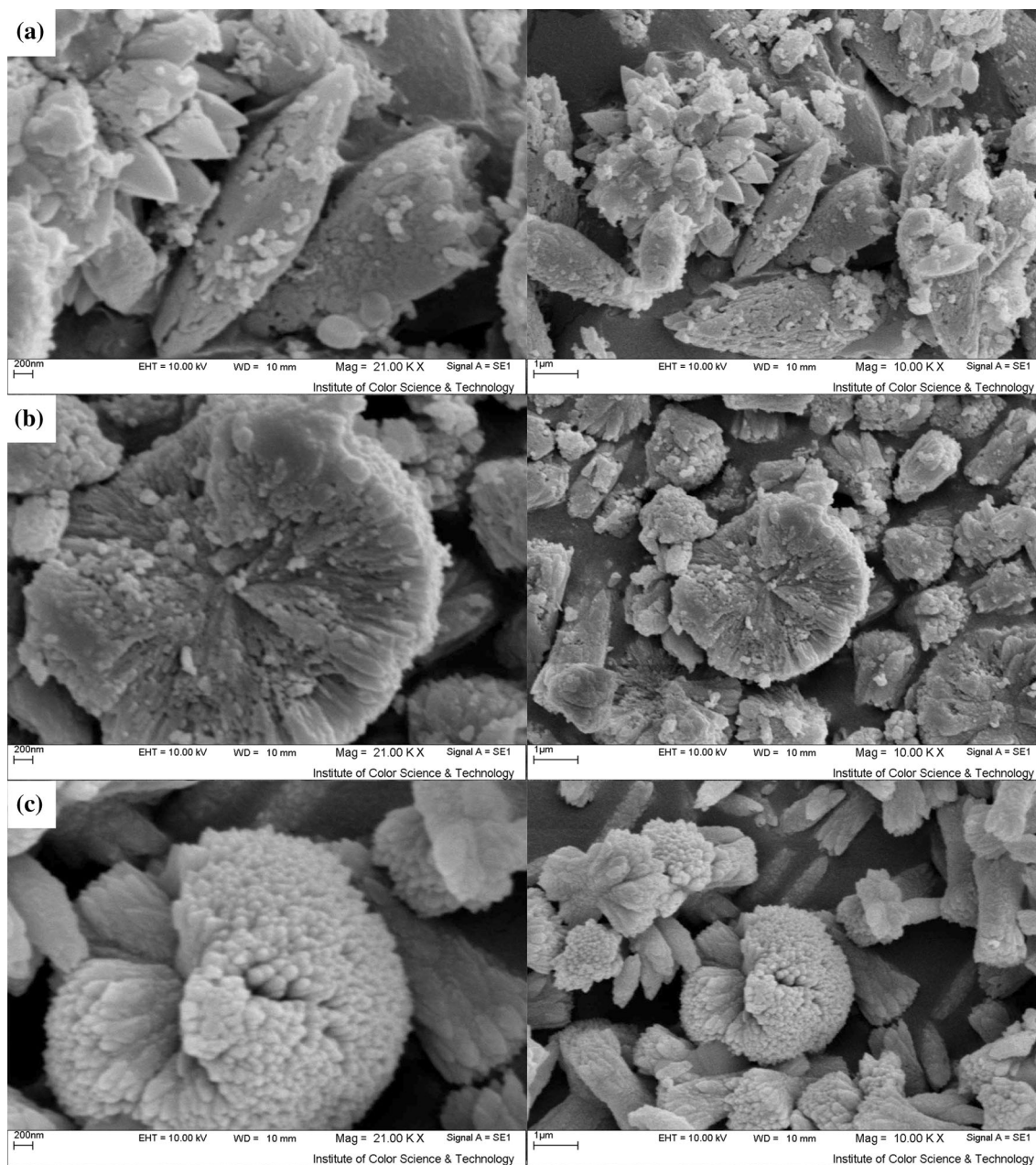


Fig. 2 SEM image of SrMoO_4 nanostructures **a** sample 1, **b** sample 2, **c** samples 3

2.3 Photocatalytic experimental

The methyl orange (MO) photodegradation was examined as a model reaction to evaluate the photocatalytic activities of the SrMoO_4 nanostructures. The photocatalytic experiments were performed under an irradiation ultraviolet light. The photocatalytic degradation was performed with 50 mL solution of methyl orange (0.0005 g) containing 0.1 g of SrMoO_4 nanostructures. This mixture was aerated for 30 min to reach adsorption equilibrium. Later, the mixture was placed inside the photoreactor in which the vessel was 15 cm away from the

ultraviolet source of 400 W mercury lamps. The photocatalytic tests were performed at room temperature. Aliquots of the mixture were taken at definite interval of times during the irradiation, and after centrifugation they were analyzed by a UV–Vis spectrometer. The methyl orange (MO) degradation percentage was calculated as:

$$\text{Degradation rate}(\%) = 100(A_0 - A_t)/A_0 \quad (1)$$

where A_t and A_0 are the obtained absorbance value of the methyl orange solution at t and 0 min by a UV–Vis spectrometer, respectively.

Fig. 3 EDS pattern of SrMoO₄ nanostructures (sample 1)

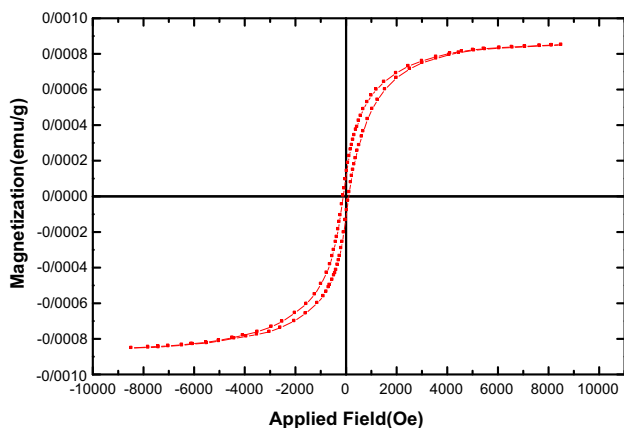
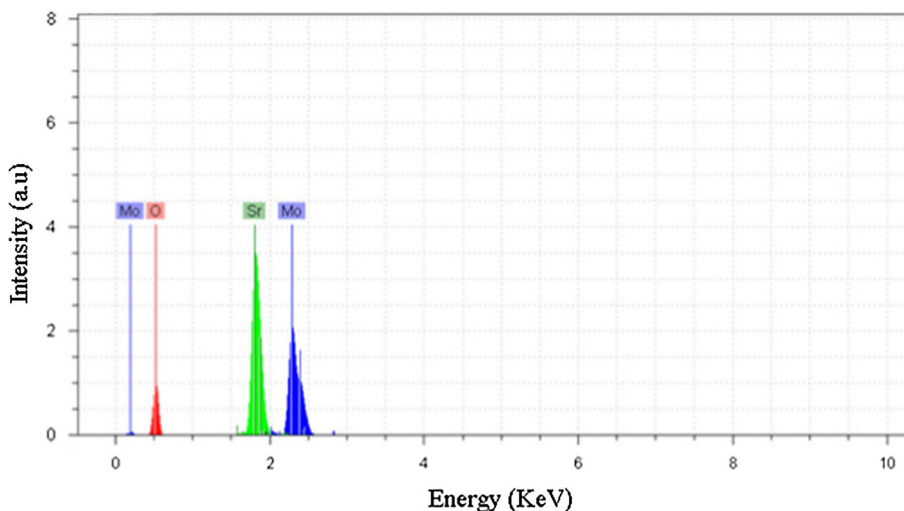


Fig. 4 VSM curve of SrMoO₄ nanostructures (sample 1)

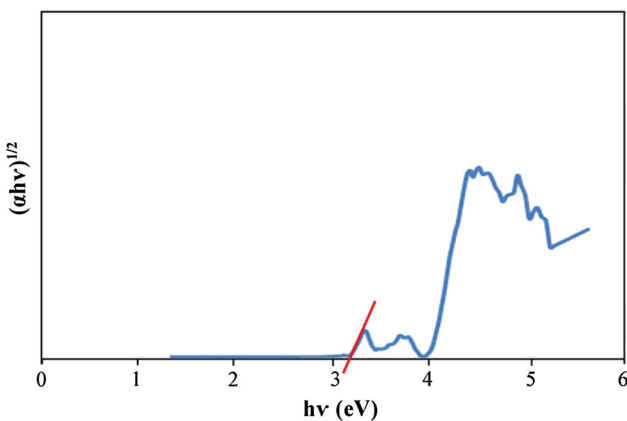


Fig. 5 UV-Vis pattern of SrMoO₄ nanostructures (sample 1)

3 Results and discussion

Crystalline structure and phase purity of as-prepared SrMoO₄ nanostructures has been determined using XRD. The XRD pattern of SrMoO₄ nanostructures (sample 1) is

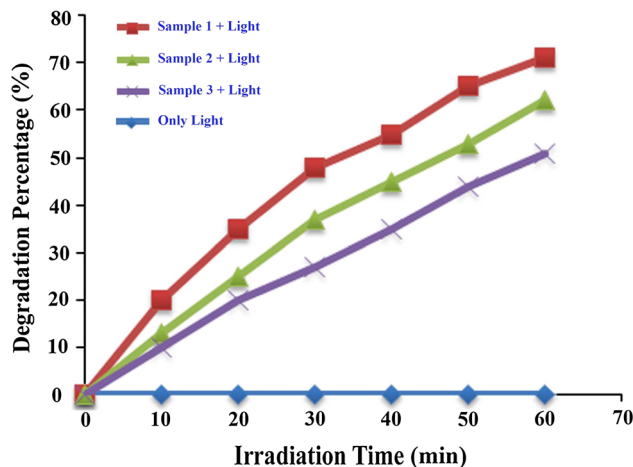


Fig. 6 Time dependent decolorization of methyl orange aqueous solutions under UV light illumination in blank and presence of the various SrMoO₄ nanostructures

shown in Fig. 1. Based on the Fig. 1, the diffraction peaks observed can be indexed to pure tetragonal phase of SrMoO₄ nanostructures ($a = b = 5.3944 \text{ \AA}$, $c = 12.0200 \text{ \AA}$) with space group of I41/a and JCPDS no. 08-0482. No diffraction peaks from other species could be detected, which indicates the obtained sample is pure. From XRD data, the crystallite diameter (D_c) of SrMoO₄ nanostructures (sample 1) was calculated to be 36 nm using the Scherer equation:

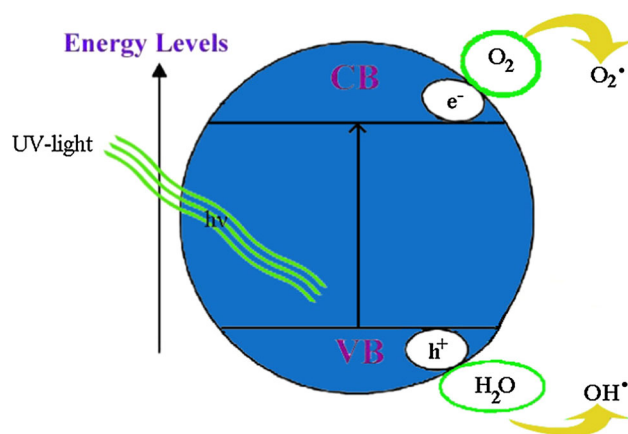
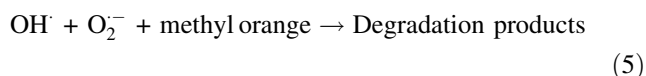
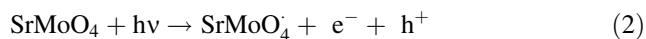
$$D_c = K\lambda/\beta\cos\theta \quad \text{Scherer equation}$$

where β is the breadth of the observed diffraction line at its half intensity maximum, K is the so-called shape factor, which usually takes a value of about 0.9, and λ is the wavelength of X-ray source used in XRD. In today's modern world natural surfactants and capping agents play a vital role in synthesis of nanomaterials especially where size and morphology of final products be very important

[33–35]. Hence, in this research we examined the effect of glucose and lactose as the capping agents on the synthesis SrMoO₄ nanostructures. In the absence of capping agents (glucose and lactose, sample 1), the product mainly consists of flower-like nanostructures which formed by almond nanostructure, as shown in Fig. 2a. According to the Fig. 2b, in the presence of lactose products consist of agglomeration sheet nanostructures. Changing capping agent from lactose to glucose causes formation flower-like nanostructures consist of nanorods, as shown in Fig. 2c. The EDS analysis measurement was used to investigate the chemical composition and purity of SrMoO₄ nanostructures (sample 1). According to the Fig. 3, the product consists of Sr, W, and O elements. Furthermore, neither N nor C signals were detected in the EDS spectrum, which means the product is pure and free of any surfactant or impurity. The VSM magnetic measurements for the SrMoO₄ Fig. 4 show the magnetic properties of nanoparticles prepared at low temperature. The SrMoO₄ nanostructures (sample 1) exhibit ferromagnetic behavior at room temperature, with a saturation magnetization of .0008 emu/g and a coercivity of 125 Oe. Figure 5 shows the diffused reflectance spectrum of the as-prepared SrMoO₄ nanostructures (sample 1). The fundamental absorption edge in most semiconductors follows the exponential law. Using the absorption data the band gap was estimated by Tauc's relationship:

$$\alpha = \alpha_0(h\nu - E_g)^n/h\nu$$

where α is absorption coefficient, $h\nu$ is the photon energy, α_0 and h are the constants, E_g is the optical band gap of the material, and n depends on the type of electronic transition and can be any value between 0.5 and 3. The energy gap of the SrMoO₄ nanostructures (sample 1) is determined by extrapolating the linear portion of the plots of $(\alpha h\nu)^2$ against $h\nu$ to the energy axis, as shown in Fig. 5. The E_g value is calculated as 3.25 eV for the SrMoO₄ nanostructures. Photodegradation of methyl orange under UV light irradiation (Fig. 6) was employed to evaluate the photocatalytic activity of the as-synthesized SrMoO₄ (sample 1–3). No methyl orange was practically broken down after 60 min under UV light irradiation in the absence of nanocrystalline SrMoO₄. The probable mechanism of the photocatalytic degradation of methyl orange can be summarized as follows:



Scheme. 1 A schematic diagram of methyl orange degradation reaction mechanism over the surface of SrMoO₄ nanostructures

Using photocatalytic calculations by Eq. (1), the methyl orange degradation was about 73, 62, and 51 % after 60 min irradiation of UV light in the presence of samples 1–3, respectively. The degradation pathway of methyl orange over the surface of SrMoO₄ nanostructures is shown in Scheme 1.

4 Conclusions

In this work, SrMoO₄ nanostructures were successfully synthesized by simple sonochemical method in an aqueous solution. EDS and XRD results proved high purity of the as-prepared SrMoO₄ nanostructures. To investigate the effect of capping agents on the morphology and size of final products several tests were performed in the presence of glucose and lactose. The products were analyzed by scanning electron microscopy (SEM), and ultraviolet–visible (UV–Vis) spectroscopy to be round, about 50–55 nm in size and $E_g = 3.25$ eV. Applying nanocrystalline SrMoO₄ as the photocatalyst causes maximum 73 % degradation of methyl orange after 60 min irradiation of UV light.

Acknowledgments Authors are grateful to council of University of Arak for providing financial support to undertake this work.

References

1. M. Ramezani, A. Sobhani-Nasab, S.M. Hosseinpour-Mashkani, J. Mater. Sci. Mater. Electron. **26**, 4848 (2015)
2. M. Ramezani, S.M. Hosseinpour-Mashkani, A. Sobhani-Nasab, H. Ghasemi-Estarki, J. Mater. Sci. Mater. Electron. **26**, 7588 (2015)
3. M. Zahraei, A. Monshi, D. Shahbazi-Gahrouei, M. Amirnasr, B. Behdadfar, M. Rostami, J. NanoStruct. **5**, 137 (2015)

4. M. Mousavi-Kamazani, M. Salavati-Niasari, D. Ghanbari, J. NanoStruct. **2**, 363 (2012)
5. F. Beshkar, M. Salavati-Niasari, J. NanoStruct. **5**, 17 (2015)
6. M. Panahi-Kalamuei, M. Mousavi-Kamazani, M. Salavati-Niasari, J. NanoStruct. **4**, 459 (2014)
7. S. Khaleghi, J. NanoStruct. **2**, 157 (2012)
8. M. Behpour, M. Mehrzad, S.M. Hosseinpour-Mashkani, J. NanoStruct. **5**, 183 (2015)
9. M. Riazian, J. NanoStruct. **4**, 433 (2014)
10. L. Nejati-Moghadam, A. Esmaili Bafghi-Karimabad, M. Salavati-Niasari, H. Safardoust, J. NanoStruct. **5**, 47 (2015)
11. E. Khosravifard, M. Salavati-Niasari, M. Dadkhah, G. Sodeifian, J. NanoStruct. **2**, 191 (2010)
12. M. Shahrekizad, A. Gholamalizadeh-Ahangar, N. Mir, J. NanoStruct. **5**, 117 (2015)
13. M. Anicete-Santos, E. Orhan, M.A. de Maurera, L.G.P. Simoes, A.G. Souza, P.S. Pizani, E.R. Leite, J.A. Varela, J. Andrés, A. Beltrán, E. Longo, Phys. Rev. B. **75**, 165105 (2007)
14. J.H. Ryu, J.W. Yoon, K.B. Shim, Solid State Commun. **133**, 657 (2005)
15. A.P.A. Marques, D.M.A. de Melo, C.A. Paskocimas, P.S. Pizani, M.R. Joya, E.R. Leite, E. Longo, J. Solid State Chem. **179**, 671 (2006)
16. A.M.E.S. Raj, C. Mallika, O.M. Sreedharan, K.S. Nagaraja, Mater. Lett. **53**, 316 (2002)
17. R. Sundaram, K.S. Nagaraja, Mater. Res. Bull. **39**, 581 (2004)
18. Z. Lou, M. Cocivera, Mater. Res. Bull. **37**, 1573 (2002)
19. I.C. Lekshmi, A. Gayen, M.S. Hegde, Mater. Res. Bull. **40**, 93 (2005)
20. A. Kaddouri, E. Tempesti, C. Mazzocchia, Mater. Res. Bull. **39**, 695 (2004)
21. H.H. Wang, D.F. Cui, Y.L. Zhou, Z.H. Chen, F. Chen, T. Zhao, H.B. Lu, G.Z. Yang, M.C. Xu, Y.C. Lan, X.L. Chen, H.J. Qian, F.Q. Liu, J. Cryst. Growth **226**, 261 (2001)
22. J.P. Chu, I.J. Hsieh, J.T. Chen, M.S. Feng, Mater. Chem. Phys. **53**, 172 (1998)
23. J. Bi, C.H. Cui, X. Lai, F. Shi, D.J. Gao, Mater. Res. Bull. **43**, 743 (2008)
24. J.C. Sczancoski, L.S. Cavalcante, M.R. Joya, J.A. Varela, P.S. Pizani, E. Longo, J. Chem. Eng. **140**, 632 (2008)
25. S.B. Mikhlin, A.N. Mishin, A.S. Potapov, P.A. Rodnyi, A.S. Voloshinovskii, Nucl. Instrum. Methods Phys. Res. A **486**, 295 (2002)
26. J. Bi, L. Wu, Y. Zhang, Z. Li, J. Li, X. Fu, Appl. Catal. B Environ. **91**, 135 (2009)
27. A.W. Sleight, Acta Crystallogr. B **28**, 2899 (1972)
28. J.C. Sczancoski, L.S. Cavalcante, M.R. Joya, J.A. Varela, P.S. Pizani, E. Longo, Chem. Eng. J. **140**, 632 (2008)
29. X. Lin, X. Qiao, X. Fan, Solid State Sci. **13**, 579 (2011)
30. Q. Wei, D. Chen, Cent. Eur. J. Phys. **8**, 766 (2010)
31. S.K. Suslik, *Ultrasound its Chemical Physical and Biological Effects* (VCH, Weinheim, 1988)
32. S. Koda, T. Kimura, T. Kondo, H. Mitome, Ultrason. Sonochem. **10**, 149 (2003)
33. Y.C. Cheng, C.C. Yu, T.Y. Lo, Y.C. Liu, Mater. Res. Bull. **47**, 1107 (2012)
34. F. Cheng, L.J. Gamble, G.V. Castner, Anal. Chem. **80**, 2564 (2008)
35. Z. Niu, Y. Li, Chem. Mater. **26**(1), 72 (2014)